



A new insight of recycling of spent Zn–Mn alkaline batteries: Synthesis of $Zn_xMn_{1-x}O$ nanoparticles and solar light driven photocatalytic degradation of bisphenol A using them



Jiao Qu^{a,b,*}, Yue Feng^a, Qian Zhang^a, Qiao Cong^{a,b,*}, Chunqiu Luo^a, Xing Yuan^b

^aSchool of Chemistry and Chemical Engineering, Bohai University, Jinzhou, Liaoning 121013, China

^bSchool of Urban and Environmental Sciences, Northeast Normal University, Changchun, Jilin 130024, China

ARTICLE INFO

Article history:

Received 26 September 2014

Received in revised form 29 October 2014

Accepted 30 October 2014

Available online 7 November 2014

Keywords:

Spent alkaline battery

$Zn_xMn_{1-x}O$

Nanoparticle

Bisphenol A

Degradation

ABSTRACT

This work focuses on the synthesis of $Zn_{0.1}Mn_{0.9}O$, $Zn_{0.3}Mn_{0.7}O$, and $Zn_{0.5}Mn_{0.5}O$ nanoparticles using Zn–Mn spent alkaline batteries (SABs) as raw materials and their applications for photocatalytic degradation of bisphenol A in water. Zn–Mn SABs were manually dismantled into scrap (including plastics, copper cap, zinc crust, and carbon rod) and powder. The mashed zinc crust and pretreated powder were successively added into H_2SO_4 and $NH_3 \cdot H_2O$, and the formed precipitates were characterized. The yield (wt) of synthesis of $Zn_{0.5}Mn_{0.5}O$ ($ZnMnO_3$) nanoparticles was 57.1%. The synthesized $Zn_{0.5}Mn_{0.5}O$ nanoparticles were cylinder, with a length of 60 nm. Afterwards, the removal efficiencies of bisphenol A (BPA) under solar light irradiation with the recovered $Zn_xMn_{1-x}O$ nanoparticles were investigated: (1) the adsorption equilibrium of BPA on $Zn_xMn_{1-x}O$ nanoparticles could be achieved after approximate 40 min. The saturation absorbance of BPA was about $32.40 \pm 4.76 \text{ mg g}^{-1}$, $20.40 \pm 3.60 \text{ mg g}^{-1}$, and $14.50 \pm 4.55 \text{ mg g}^{-1}$ by $Zn_{0.1}Mn_{0.9}O$, $Zn_{0.3}Mn_{0.7}O$, and $Zn_{0.5}Mn_{0.5}O$ nanoparticles, respectively; (2) compared with the $21.7 \pm 1.6\%$ degradation of BPA (only solar light irradiation for 180 min), the combination of solar light irradiation and $Zn_{0.1}Mn_{0.9}O$, $Zn_{0.3}Mn_{0.7}O$, and $Zn_{0.5}Mn_{0.5}O$ nanoparticles could lead to $59.41 \pm 4.32\%$, $83.43 \pm 2.73\%$, and $71.22 \pm 4.79\%$ decomposition yields of BPA, respectively. These findings have positive effects on solving the recycling of SABs, decreasing the cost of catalysts, and the problem of organic pollutant in water.

© 2014 Elsevier B.V. All rights reserved.

1. Introduction

Zn–Mn alkaline batteries are usually used by the portable electronic devices requiring small electric power, such as radios, remote controls, cameras, and toys [1–3]. Since 2002, more than 15 billion Zn–Mn batteries have been produced annually in China [4]. Moreover, the world-wide consumption of batteries is also significant. Most of the spent alkaline batteries (SABs) are discarded as waste, although the SABs are classified as hazardous waste. Thus, the recycling of wasted batteries is significant not only to environmental safety and human health, but also in economical point of view to resource and materials.

To solve environmental problems and utilize secondary material resources, a great effort has been made to recycle the SABs in the last two decades [5,6]. However, the recycling with an

unadorned purpose of waste treatment is not an attractive business, particularly in developing countries where economic interests supersede environmental obligations. Some researchers have proposed the separation of valuable metals from Zn–Mn SABs with the application of phosphonic acid, phosphinic acid extractants, and trialkyl phosphine oxides [7]. Nevertheless, it is considered that these processes are not predominant for reducing the recycling cost. Most recovery of valuable metals from SABs is generally carried out by precipitation and thermal treatments via ammoniacal or acidic leaching processes to yield reusable oxides or ferrites [8–10]. Most of the methods of recovering valuable metal components from SABs do not necessarily catch the fancy due to limited applicability and low commercial value of the end product.

Recently, using SABs as raw materials to synthesize Zn–Mn ferrite magnetic materials has been developed owing to the presence of adequate amounts of Mn, Zn, and Fe in them. Zn–Mn ferrites are extensively used in transformers, electromagnetic gadgets, information storage systems, and biomedical devices because of their high magnetic permeability, saturation magnetization, dielectric

* Corresponding authors at: School of Chemistry and Chemical Engineering, Bohai University, Jinzhou, Liaoning 121013, China. Tel.: +86 416 3400047; fax: +86 416 3400161.

E-mail address: qujiao@bhu.edu.cn (J. Qu).

resistivity and relatively low eddy current losses [11,12]. However, it is worthy to note that the reactant contents have to be adjusted with lots of pure reagent when SABs were directly used as precursors. In addition, the synthetic process also affects the performance of Zn–Mn ferrites [13].

In our previous work, nano materials were successfully synthesized using some plants [14–17], which could enhance the efficiencies of photocatalytic degradation on organic pollutant in water [18–32]. In this work, a convenient synthesis of $Zn_xMn_{1-x}O$ nanoparticles using Zn–Mn SABs was reported and the removal efficiencies of bisphenol A (BPA, an endocrine disruptor) under solar light irradiation with them were investigated. These findings cannot only reduce the cost and simplify the synthesis process of $Zn_xMn_{1-x}O$ nanoparticles, but also have positive effects on solving the recycling of SABs as well as the problem of organic pollutant in water.

2. Material and methods

2.1. Materials

The AA size Zn–Mn SABs (1.5 V) with the same brand and type, used in this work, were kindly provided by student association named “Sons of Earth” of Bohai university. The Zn–Mn batteries involved the mass trademarks consumed in China. The Zn–Mn SABs used in this work was weighed and the contents of main heavy metals in them were determined using atomic absorption spectrometer after being digested in aqua regia. The reagents and solvents were A. R. grade materials.

2.2. Pretreatment of SABs and elemental composition

Zn–Mn SABs were disassembled in following steps: (1) SABs were manually dismantled into scrap (including plastics, copper cap, zinc crust, and carbon rod) and powder; (2) the powder was added into 150 ml of 0.5 mol L⁻¹ sulfuric acid (H₂SO₄) and filtrated after being dried (400 °C) for 2 h, crushed, and washed many times with water; (3) 0.5 mol L⁻¹ ammonia (NH₃·H₂O) solution was added into the above mixture solution (adjust the pH values to 8.0) and filtrated; and (4) the filtrate was added into 20 ml of 2.5 mol L⁻¹ thermal sodium hydroxide (NaOH) solution, filtrated, and the formed black residues were collected.

2.3. Synthesis and characterization of $Zn_xMn_{1-x}O$ nanoparticles

The mashed zinc crust (the weight was about 4 g) of a set of Zn–Mn SABs and the above black residues were added into 1.25 mol L⁻¹ H₂SO₄ solution containing 2.5 wt% hydrogen peroxide (H₂O₂) with magnetic stirring at 85 °C until complete dissolution [33]. Then, the 0.5 mol L⁻¹ NH₃·H₂O was added into the mixture to adjust the pH to 8.5 at 85 °C. The precipitates were filtered after aging for 3 h at 85 °C, washed, and dried at 500 °C for 2 h.

The synthesized $Zn_xMn_{1-x}O$ nanoparticles were characterized by the follow methods: X-ray diffraction (XRD) pattern was obtained on a Rigaku D-max C III (Ni-filtered Al K α radiation); scanning electron microscopy (SEM) image was performed using a JEOL JSM-840 operated at 3.0 kV; energy dispersive spectrum (EDS) was obtained using an Oxford EDX system attached to SEM.

In addition, 1 g and 2.5 g mashed zinc crust of Zn–Mn SABs were also used to synthesize $Zn_xMn_{1-x}O$ nanoparticles (different proportions of Zn and Mn) in accordance with the above processes.

2.4. Adsorption and photodegradation experiment

The experimental procedure for the adsorption/desorption and photocatalytic degradation of BPA under solar light irradiation was carried out as follows: (1) 10 mg synthesized $Zn_xMn_{1-x}O$ (different proportions of Zn and Mn) nanoparticles were added into 100 mL aqueous solution of BPA (10 mg L⁻¹), respectively. After continuously stirred and kept in the dark at 25 °C, the supernatant was collected at different time intervals; (2) 10 mg L⁻¹ BPA (100 mL) solution were added in a pyrex cylindrical vessel and continuously stirred under the solar light irradiation (using a solar simulator, 150 W Xenon) for 180 min to evaluate the photodegradation capacities. The distance between the photosource and reactor was 10 cm. At different time intervals, the supernatant was collected; (3) 10 mg L⁻¹ BPA (100 mL) solution and 10 mg $Zn_xMn_{1-x}O$ nanoparticles (different proportions of Zn and Mn) were added in a pyrex cylindrical vessel. After equilibration of adsorption/desorption for BPA on the surfaces of $Zn_xMn_{1-x}O$ nanoparticles was completed in the darkness, the resulted suspensions were continuously stirred under the solar light irradiation for 180 min. The distance between the photosource and reactor was 10 cm. At different time intervals, the supernatant was collected; and (4) the collected supernatant was centrifuged at 5000 rpm for 30 min in the centrifuge.

The BPA concentrations were determined by high performance liquid chromatography (HPLC) after the supernatant was filtered through 0.22 mm Millipore cellulose acetate membrane. In the experiments, three replicates were carried out.

3. Results and discussion

3.1. Composition of Zn–Mn SABs

The weight of a set of Zn–Mn SABs used in this work was 24 g. The composition of main metals in Zn–Mn SABs (Table 1) was shown as follows: 15.5 ± 2.13% for Zn, 26.7 ± 6.24% for Mn, 0.004 ± 0.001% for Hg, 0.01 ± 0.002% for Cd, 8.52 ± 0.07% for Fe, 0.32 ± 0.11% for Pb, 1.62 ± 0.18% for Cu.

3.2. Characterization of $Zn_xMn_{1-x}O$ nanoparticles

Fig. 1 showed XRD pattern of the synthesized $Zn_xMn_{1-x}O$ nanoparticles from Zn–Mn SABs (the dosage of zinc crust was 4 g). All the diffraction peaks could be well indexed to the hexagonal phase ZnMnO₃ reported in JCPDS card (No. 19-1461). Furthermore, the broadening at the bottom of diffraction peaks also denoted that the crystalline sizes were small, and the diffraction peaks were narrow, which meant that crystalline substances were synthesized [34].

In the EDS spectrum (Fig. 2) of the synthesized $Zn_xMn_{1-x}O$, the peaks of Zn, Mn, and O were obviously observed. The atom fractions of Zn and Mn were 15.04% and 14.93%, and the ratio of Zn to Mn was nearly 1:1. So, the Zn_{0.5}Mn_{0.5}O nanoparticles were synthesized, and it was proposed that the synthesized Zn_{0.5}Mn_{0.5}O were corresponding to the ZnMnO₃ (ZnO and MnO₂) structure. In addition, the weight of the synthesized Zn_{0.5}Mn_{0.5}O nanoparticles was 13.7 g from a set of Zn–Mn SABs, it meant that the yield was 57.1%.

As shown in Table 1, there were Hg, Cd, Fe, Pb, and Cu in the Zn–Mn SABs. However, our synthesized Zn_{0.5}Mn_{0.5}O nanoparticles from Zn–Mn SABs did not include any impurities. The other metals were removed in the process of synthesis of SABs: (1) the Hg was volatilized in the dry process (400 °C) for 2 h [3]; (2) the Pb was formed to PbSO₄ (precipitation) with H₂SO₄ and removed by filtration; (3) the Cd was formed to Cd(OH)₂ (precipitation) under the condition of the pH values at 8.0 and removed by filtration, but the Mn(OH)₂ was dissolved in solutions containing ammonium salts [35]; and (4) the Fe was dissolved in thermal NaOH solution, but undissolved Mn(OH)₂ was collected.

To obtain more details of the Zn_{0.5}Mn_{0.5}O nanoparticles structure from Zn–Mn SABs, the structures of residual frameworks were characterized by SEM (shown in Fig. 3). The SEM image confirmed that the Zn_{0.5}Mn_{0.5}O nanoparticles were polydispersed rather than in uniform distribution. The synthesized Zn_{0.5}Mn_{0.5}O nanoparticles were cylinder, and the length of the them was 60 nm.

Afterwards, with the additions of the 1 g and 2.5 g mashed zinc crust of Zn–Mn SABs, the Zn_{0.1}Mn_{0.9}O and Zn_{0.3}Mn_{0.7}O nanoparticles

Table 1
Composition of main metals in Zn–Mn SABs (%).

Metals	Percentage
Zn	15.5 ± 2.13 ^b
Mn	26.7 ± 6.24 ^b
Hg	0.004 ± 0.001 ^b
Cd	0.01 ± 0.002 ^b
Fe	8.52 ± 0.07 ^a
Pb	0.32 ± 0.11 ^b
Cu	1.62 ± 0.18 ^b

The percentages of other elements were not shown. Data were average ± S.E, n = 3.

^a Significant at P < 0.01.

^b Significant at P < 0.05.

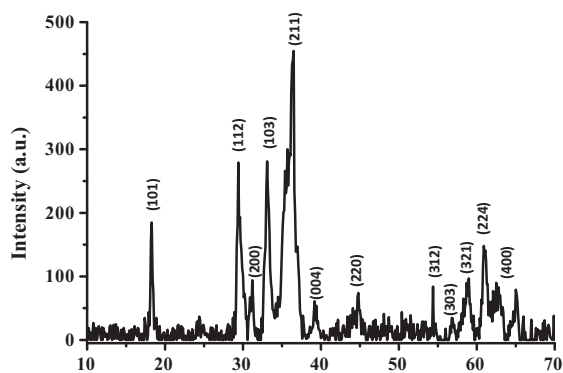


Fig. 1. XRD pattern of synthesized $Zn_{0.5}Mn_{0.5}O$ nanoparticles.

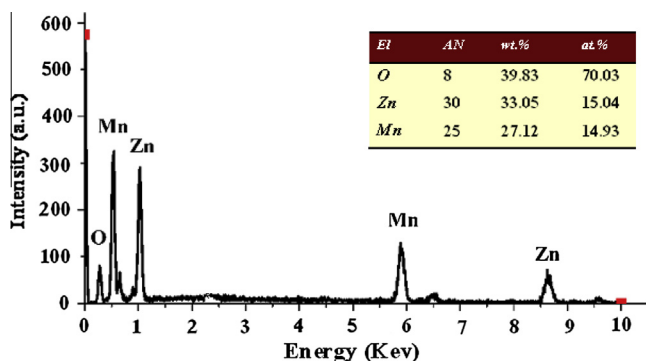


Fig. 2. EDS spectrum of synthesized $Zn_{0.5}Mn_{0.5}O$ nanoparticles.

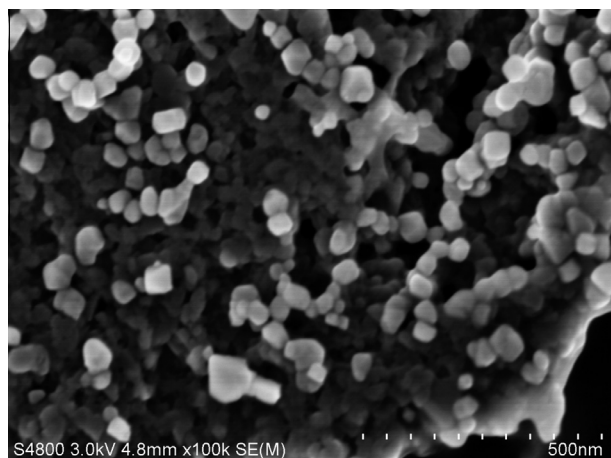


Fig. 3. SEM image of synthesized $Zn_{0.5}Mn_{0.5}O$ nanoparticles.

(characterization no shown) were also synthesized using Zn–Mn SABS.

3.3. Effect of synthesized $Zn_xMn_{1-x}O$ nanoparticles on adsorption and photodegradation of BPA

Fig. 4 showed the adsorption kinetic curves of BPA (100 mL, initial concentration of BPA was 10 mg L^{-1}) on $Zn_xMn_{1-x}O$ nanoparticles. The adsorption equilibriums of BPA on $Zn_{0.1}Mn_{0.9}O$, $Zn_{0.3}Mn_{0.7}O$, and $Zn_{0.5}Mn_{0.5}O$ nanoparticles could be achieved in a short time (approximately 40 min), it meant that $Zn_xMn_{1-x}O$ nanoparticles were very effective sorbents for BPA. From Table 2, the saturation absorbance of BPA was about $32.40 \pm 4.06 \text{ mg g}^{-1}$,

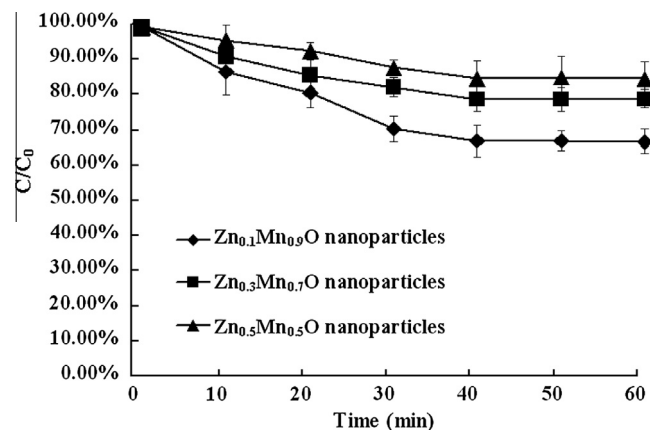


Fig. 4. Adsorption kinetic curves of BPA on $Zn_xMn_{1-x}O$ nanoparticles at 25°C .

$20.40 \pm 3.60 \text{ mg g}^{-1}$, and $14.50 \pm 4.55 \text{ mg g}^{-1}$ ($32.40 \pm 4.06\%$, $20.40 \pm 3.60\%$, and $14.50 \pm 4.55\%$) by $Zn_{0.1}Mn_{0.9}O$, $Zn_{0.3}Mn_{0.7}O$, and $Zn_{0.5}Mn_{0.5}O$ nanoparticles, respectively. In addition, the effects of the synthesized $Zn_xMn_{1-x}O$ nanoparticles on adsorption of BPA were increased with the increasing proportions of Mn in $Zn_xMn_{1-x}O$ nanoparticles. Manganese dioxides were poor crystalline oxides exhibiting large adsorption capacities, owing to their varying tunnel structures and large specific surface areas [36]. It is proposed that the main effect of MnO_2 , with large surface area, on BPA was adsorption.

Photolysis (only solar light irradiation) and photocatalysis (solar light irradiation and addition with $Zn_xMn_{1-x}O$ nanoparticles) of degradation of BPA by $Zn_xMn_{1-x}O$ nanoparticles were investigated (Fig. 5). Irradiated with solar light for 180 min, the degradation of BPA (10 mg L^{-1}) was $21.7 \pm 1.6\%$. As shown in Table 2, the combination of solar light irradiation (180 min) and the synthesized $Zn_{0.1}Mn_{0.9}O$, $Zn_{0.3}Mn_{0.7}O$, and $Zn_{0.5}Mn_{0.5}O$ nanoparticles from Zn–Mn SABS could result in $59.41 \pm 4.32\%$, $83.43 \pm 2.73\%$, and $71.22 \pm 4.79\%$ decomposition yields of BPA, respectively. These results demonstrated that the photodegradation rate of BPA solutions with the presence of $Zn_{0.3}Mn_{0.7}O$ nanoparticles was much faster than those containing $Zn_{0.1}Mn_{0.9}O$ and $Zn_{0.5}Mn_{0.5}O$ nanoparticles. In the photocatalytic oxidation process, organic pollutants were destroyed in the presence of semiconductor photocatalysts (ZnO), an energetic light source, and an oxidizing agent such as oxygen or air [37].

The nanoparticles have the tiny size and large volume percentage on surface. The band state and electronic state on the surface of nanoparticles differ from the states of inner. The atomic complexing state is not perfect on the surface of nanoparticles. These special properties could lead to the increase of active positions on the surface. As the size of nanoparticles is reduced, the roughness of the surface aggravates and the rough atomic steps are formed, which could result in the increase of absorption ability and contacting area for chemical reaction [38]. In addition, the quantum effects of the $Zn_xMn_{1-x}O$ nanoparticles converted the energy levels of conduction band and valence band into splitting energy levels. Therefore, the electrons of $Zn_xMn_{1-x}O$ nanoparticles are excited from valence band to conduction band after solar illumination, and the holes are formed in the valence band (h^+). Hole itself is a strong oxidant. It could oxidize the OH^- and H_2O_2 absorbed on the $Zn_xMn_{1-x}O$ nanoparticles surfaces to form the free radical of OH^\cdot . The radical of OH^\cdot combined on $Zn_xMn_{1-x}O$ nanoparticles surfaces is a strong oxidant, and it could not only oxidize the adjacent organic compounds, but also being diffused into the solution.

ZnO is an important member in the II–VI group semiconductors with a wide bandgap (3.37 eV), however, the wide bandgap of

Table 2
Removal efficiencies of BPA by $Zn_xMn_{1-x}O$ nanoparticles (%).

Time (min)	Adsorption					Photocatalysis					
	10	20	30	40	50	60	30	60	90	120	180
$Zn_{0.1}Mn_{0.9}O$	12.41 ± 4.87 ^b	18.12 ± 3.78 ^b	28.31 ± 3.52 ^b	32.40 ± 4.06 ^b	32.38 ± 1.07 ^a	32.40 ± 2.09 ^a	36.12 ± 5.22 ^b	40.13 ± 4.85 ^b	48.11 ± 3.37 ^a	54.63 ± 1.51 ^a	59.41 ± 4.32 ^a
$Zn_{0.3}Mn_{0.7}O$	8.12 ± 1.84 ^b	14.23 ± 2.56 ^b	15.96 ± 0.79 ^a	20.40 ± 3.60 ^b	20.39 ± 3.72 ^b	20.40 ± 0.53 ^a	42.28 ± 1.29 ^a	56.17 ± 2.13 ^a	65.04 ± 2.71 ^a	74.03 ± 5.03 ^a	83.43 ± 2.73 ^a
$Zn_{0.5}Mn_{0.5}O$	4.83 ± 2.69 ^b	8.02 ± 0.35 ^a	12.94 ± 0.27 ^b	14.50 ± 4.55 ^b	14.51 ± 5.71 ^b	14.50 ± 4.06 ^b	26.34 ± 4.57 ^b	48.32 ± 2.24 ^a	57.89 ± 2.69 ^a	64.93 ± 2.73 ^a	71.22 ± 4.79 ^a

Data were average ± S.E, $n = 3$.

^a Significant at $P < 0.01$.

^b Significant at $P < 0.05$.

MnO_2 is only 1.30 eV [39]. Consequently, the photocatalytic performance of ZnO was better than that of MnO_2 upon combination with solar light irradiation. The previous research results indicated that oxidative reactions with ZnO may play an important role in the fate of BPA [40]. The formation of dimeric products via oxidative coupling and monomeric products via hydroxylation and dealkylation of BPA were the major reaction mechanisms in

the oxidation of BPA by ZnO. Compared with $Zn_{0.3}Mn_{0.7}O$ and $Zn_{0.5}Mn_{0.5}O$ nanoparticles, the photocatalytic active sites were minimum due to the fact that the content of Zn in $Zn_{0.1}Mn_{0.9}O$ nanoparticles was least. Therefore, the photodegradation rate of BPA solutions with $Zn_{0.1}Mn_{0.9}O$ nanoparticles was lowest. In theory, the decomposition yields of BPA might be increased with the increasing of proportions of Zn in $Zn_xMn_{1-x}O$ nanoparticles. Thus, $Zn_{0.5}Mn_{0.5}O$ nanoparticles might show the fastest photodegradation rate of BPA. However, photodegradation rate of BPA by $Zn_{0.3}Mn_{0.7}O$ nanoparticles was much faster than that of by $Zn_{0.5}Mn_{0.5}O$ nanoparticles.

However, both Zn and Mn, present as background electrolytes, decreased the reaction rates possibly because of their adsorption and blocking of active sites on the MnO_2 and ZnO surfaces [41]. The reaction mechanisms for the photodegradation of BPA using $Zn_xMn_{1-x}O$ nanoparticles were similar, and since the pre-adsorption of the target on the surface of catalyst was prerequisite for enhancement of photodegradation and due to their adsorption abilities [42,43]. MnO_2 could adsorb the BPA, as a result, the degradation of BPA was enhanced and the better photocatalytic activity of $Zn_{0.3}Mn_{0.7}O$ nanoparticles was confirmed. As for the $Zn_xMn_{1-x}O$ nanoparticles, MnO_2 acted as a photo generated electron acceptor to promote interfacial electron transfer processes from the attached ZnO to the MnO_2 . In case of composite structures, the ZnO tips were capped by MnO_2 which reduced slightly surface to volume ratio decreasing the band bending and slightly reducing the surface defects by reducing free exciton-longitudinal optical

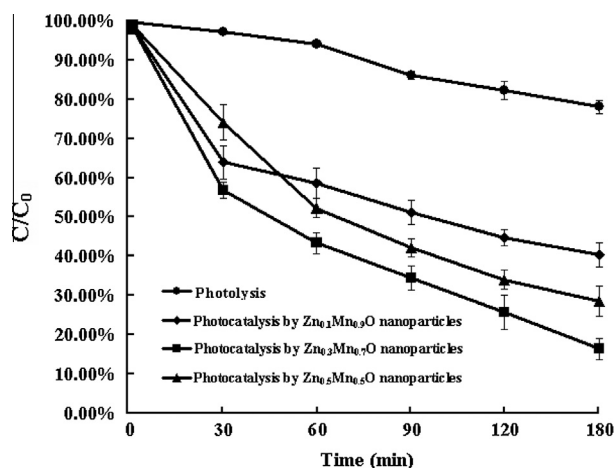


Fig. 5. Degradation of BPA by photolysis and photocatalysis.

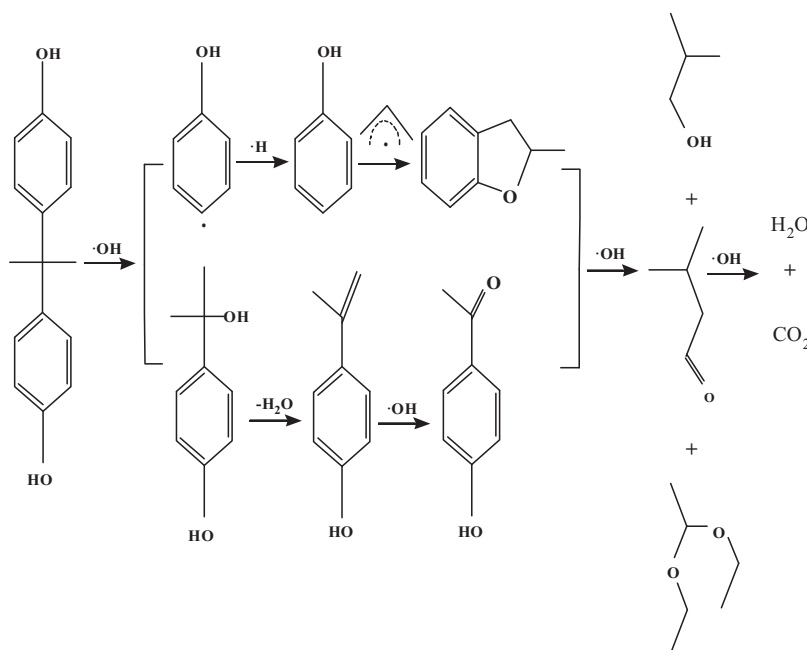


Fig. 6. Proposed degradation mechanism of BPA.

phonon interaction which resulted in slight blue shift in the composite structures [44]. In $Zn_xMn_{1-x}O$ nanoparticles, the charge carriers in the conduction band of ZnO were transferred into the MnO_2 which was very fast process that helps in less charge trapping at the grain boundaries, thereby resulting in the sharper emission peaks [45]. The recombination of photoinduced electron and hole would be retarded. Compared with the $Zn_{0.5}Mn_{0.5}O$ nanoparticles, the photocatalytic property of $Zn_{0.3}Mn_{0.7}O$ nanoparticles was improved.

The possible degradation path way (shown in Fig. 6) for BPA could be proposed as follows: 4-(1-hydroxy-1-methyl-ethyl)-phenol (HMEP) and phenol were initially produced via the photocleavage of phenyl groups by $\cdot OH$ radical attack. 4-Vinyl-phenol was then generated by dehydration from HMEP, which was subsequently converted to 4-hydroxyacetophenone by means of oxidation. Furthermore, 2-methyl-2,3-dihydrobenzofuran could be produced from phenol. Eventually, an oxidative ring-opening reaction occurring at $C=C$ bond between the adjacent hydroxyl or ketone groups led to the formation of aliphatic compounds, such as $C_4H_{10}O$, $C_5H_{10}O$, and $C_6H_{14}O_2$, followed by mineralization to CO_2 gas. These analytical results were consistent with those reported in literature [46,47].

4. Conclusion

The present work demonstrated the synthesis of $Zn_xMn_{1-x}O$ nanoparticles using Zn–Mn SABS. The synthesized $Zn_xMn_{1-x}O$ nanoparticles were characterized by XRD, SEM, and EDS. Afterwards, the removal efficiencies of BPA under solar light irradiation by using the recovered $Zn_xMn_{1-x}O$ nanoparticles were also investigated. It was found that: (1) the synthesized $Zn_{0.5}Mn_{0.5}O$ nanoparticles were cylinder, with a length of 60 nm; (2) the adsorption equilibrium of BPA on $Zn_xMn_{1-x}O$ nanoparticles could be achieved in approximately 40 min; (3) the degradation of BPA with only solar light irradiation for 180 min was $21.7 \pm 1.6\%$, but the combination of solar light irradiation and $Zn_{0.1}Mn_{0.9}O$, $Zn_{0.3}Mn_{0.7}O$, and $Zn_{0.5}Mn_{0.5}O$ nanoparticles could lead to $59.41 \pm 4.32\%$, $83.43 \pm 2.73\%$, and $71.22 \pm 4.79\%$ decomposition yields of BPA, respectively.

Acknowledgments

The authors would like to acknowledge the financial support from the National Natural Science Foundation of China (51479005 and 51309013), and Liaoning Science and Public Research Fund (2012001001).

References

- [1] M.F. Almeida, S.M. Xara, J. Delgado, C.A. Costa, *Waste Manage.* 26 (2006) 466–476.
- [2] M.F. Almeida, S.M. Xara, J. Delgado, C.A. Costa, *Waste Manage.* 29 (2009) 342–349.
- [3] E. Sayilgan, T. Kukrer, G. Civelekoglu, F. Ferella, A. Akcil, F. Veglio, M. Kitis, *Hydrometallurgy* 97 (2009) 158–166.

- [4] J. Nan, D. Han, M. Cui, M. Yang, L. Pan, *J. Hazard. Mater.* 133 (2006) 257–261.
- [5] Y.A. El-Nadi, J.A. Daoud, H.F. Aly, *J. Hazard. Mater.* 143 (2007) 328–334.
- [6] K. Huang, J. Li, Z. Xu, *Waste Manage.* 30 (2010) 2292–2298.
- [7] A. Deep, K. Kumar, P. Kumar, A.L. Sharma, B. Gupta, L.M. Bharadwaj, *Environ. Sci. Technol.* 45 (2011) 10551–10556.
- [8] L. Xiao, T. Zhou, J. Meng, *Particuology* 7 (2009) 491–495.
- [9] E. Sayilgan, T. Kukrer, N.O. Yigit, G. Civelekoglu, M. Kitis, *J. Hazard. Mater.* 173 (2010) 137–143.
- [10] G. Senanayake, S.M. Shin, A. Senaputra, A. Winn, D. Pugaev, J. Avraamides, J.S. Sohn, D.J. Kim, *Hydrometallurgy* 105 (2010) 36–41.
- [11] T. Kanemaru, T. Iwasaki, S. Suda, T. Kitagawa, United States Patent (1998).
- [12] G.X. Xi, L. Yang, M. Lu, *Mater. Lett.* 60 (2006) 3582–3585.
- [13] S.B. Sang, H.L. Huang, Y.Y. Gu, Chin. *J. Nonferrous Met.* 13 (2003) 1041–1045.
- [14] J. Qu, X. Yuan, X.H. Wang, P. Shao, *Environ. Pollut.* 159 (2011) 1783–1788.
- [15] J. Qu, C.Q. Luo, Q. Cong, X. Yuan, *Environ. Chem. Lett.* 10 (2012) 153–158.
- [16] J. Qu, Q. Cong, C.Q. Luo, X. Yuan, *RSC Adv.* 3 (2013) 961–965.
- [17] J. Qu, C.Q. Luo, X. Yuan, *Environ. Sci. Pollut. Res.* 20 (2013) 3688–3695.
- [18] V.K. Gupta, R. Jain, A. Mittal, T.A. Saleh, A. Nayak, S. Agarwal, S. Sikarwar, *Mater. Sci. Eng. C* 32 (2012) 12–17.
- [19] T.A. Saleh, V.K. Gupta, *Environ. Sci. Pollut. Res.* 19 (2012) 1224–1228.
- [20] V.K. Gupta, S.K. Srivastava, D. Mohan, S. Sharma, *Waste Manage.* 17 (1997) 517–522.
- [21] A. Mittal, J. Mittal, A. Malviya, D. Kaur, V.K. Gupta, *J. Colloid Interf. Sci.* 342 (2010) 518–527.
- [22] A. Mittal, D. Kaur, A. Malviya, J. Mittal, V.K. Gupta, *J. Colloid Interf. Sci.* 337 (2009) 345–354.
- [23] A. Mittal, J. Mittal, A. Malviya, V.K. Gupta, *J. Colloid Interf. Sci.* 340 (2009) 16–26.
- [24] V.K. Gupta, S. Agarwal, T.A. Saleh, *J. Hazard. Mater.* 185 (2011) 17–23.
- [25] V.K. Gupta, I. Ali, T.A. Saleh, A. Nayak, S. Agarwal, *RSC Adv.* 2 (2012) 6380–6388.
- [26] A. Mittal, J. Mittal, A. Malviya, V.K. Gupta, *J. Colloid Interf. Sci.* 344 (2010) 495–507.
- [27] V.K. Gupta, R. Jain, A. Nayak, S. Agarwal, M. Shrivastava, *Mater. Sci. Eng. C* 31 (2011) 1062–1067.
- [28] V.K. Gupta, A. Nayak, *Chem. Eng. J.* 180 (2012) 81–90.
- [29] T.A. Saleh, V.K. Gupta, *J. Colloid Interf. Sci.* 371 (2012) 101–106.
- [30] H. Khani, M.K. Rofouei, P. Arab, V.K. Gupta, Z. Vafaei, *J. Hazard. Mater.* 183 (2010) 402–409.
- [31] S. Karthikeyan, V.K. Gupta, R. Boopathy, A. Titus, G. Sekaran, *J. Mol. Liquids* 173 (2012) 153–163.
- [32] A.K. Jain, V.K. Gupta, A. Bhatnagar, Suhas, *Sep. Sci. Technol.* 38 (2003) 463–481.
- [33] P. Hua, D.A. Pan, S.G. Zhang, J.J. Tian, A.A. Volinsky, *J. Alloys Comp.* 509 (2011) 3991–3994.
- [34] C.C. Chen, P. Liu, C.H. Lu, *Chem. Eng. J.* 144 (2008) 509–513.
- [35] A.S. Vorokh, N.S. Kozhevnikova, A.A. Uritskaya, A. Magerl, *Russ. J. Phys. Chem. A* 82 (2008) 1132–1137.
- [36] C.X. Liu, J. Wang, J.R. Tian, L. Xiang, *J. Nanomater.* doi: <http://dx.doi.org/10.1155/2013/389634>.
- [37] S. Ahmed, M.G. Rasul, W.N. Martens, R.J. Brown, M.A. Hashib, *Desalination* 261 (2010) 3–18.
- [38] S.W. Ding, L.Y. Wang, S.Y. Zhang, Q.X. Zhou, Y. Ding, S.J. Liu, Y.C. Liu, Q.Y. Kang, *Sci. China Chem.* 46 (2003) 542–548.
- [39] Y.L. Chan, S.Y. Pung, N.S. Hussain, S. Sreekantan, F.Y. Yeoh, *Mater. Sci. Forum* 756 (2013) 167–174.
- [40] Y. Tao, Z.L. Cheng, K.E. Ting, X.J. Yin, *J. Environ. Sci. Eng. A* 1 (2012) 187–194.
- [41] N. Gao, J.W. Hong, Z.Q. Yu, P.A. Peng, W.L. Huang, *Soil Sci.* 176 (2011) 265–272.
- [42] J. Zhao, T. Wu, K. Wu, K. Oikawa, H. Hidaka, N. Serpone, *Environ. Sci. Technol.* 32 (1998) 2394–2400.
- [43] V.K. Gupta, R. Jain, S. Agarwal, M. Shrivastava, *Colloid Surf. A* 378 (2011) 22–26.
- [44] C.H. Ahn, S.K. Mohanta, N.E. Lee, H.K. Cho, *Appl. Phys. Lett.* 94 (2009) 261904.
- [45] I. Robel, B.A. Bunker, P.V. Kamat, *Adv. Mater.* 17 (2005) 2458–2463.
- [46] Y. Ohko, I. Ando, C. Niwa, T. Tatsuma, T. Yamamura, T. Nakashima, Y. Kubota, A. Fujishima, *Environ. Sci. Technol.* 35 (2001) 2365–2368.
- [47] S. Fukahori, H. Ichiura, T. Kitaoka, H. Tanaka, *Appl. Catal. B–Environ.* 46 (2003) 453–462.